Agricultural and Forest Meteorology 342 (2023) 109732

Contents lists available at ScienceDirect

Agricultural and Forest Meteorology

journal homepage: www.elsevier.com/locate/agrformet

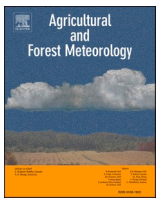

How will increased atmospheric CO_2 and climate change-induced wind trends alter the probability of tree failures from wind gusts

Samuel Woolsey *, Horia Hangan, Hassan Peerhossaini, Danielle Way

Western University, 1151 Richmond St, London, ON N6A 3K7, Canada

ARTICLE INFO

Keywords:
Wind damage modelling
Climate change
Risk
Resilience
Tree damage
Tree crown aerodynamics

ABSTRACT

Trees provide numerous benefits to communities, but pose a risk when they are damaged. The likelihood that trees will be damaged in a windstorm is increasing due to climate change, as wind trends are changing as the climate warms, and rising atmospheric CO_2 concentrations could alter the resistance of trees to wind damage.

To address these concerns, we created a tree damage model that integrates results from a meta-analysis about the effects of elevated CO_2 concentrations on tree growth and an analysis of the return period of damaging winds in Toronto, Canada from 1990 to 2080. This joint analysis is applied for a simulated silver birch (*Betula pendula*) tree. Our model predicts that by 2080, due both to a high CO_2-induced decrease in tree resilience and an increased likelihood of more frequent and intense windstorms, damaging windstorms will occur about twice as frequently as they do today.

1. Introduction

Trees provide environmental, economic and psychological benefits to their surrounding communities (Chiesura, 2004). However, trees also pose significant risks since damaged trees can cause serious harm to people and infrastructure by falling on sidewalks, roads, or power lines. More than 600 insurance claims are made against the city of Toronto each year due to fallen trees and branches causing property damage (Taylor, 2022). Tree failure can be caused by wind in two ways: (1) overturning, where the roots are pulled from the ground and the tree topples over, or (2) trunk rupture, where the trunk of the tree cannot support the load applied by the wind, and the trunk is broken. To mitigate tree failure, arborists estimate the likelihood of a failure event for trees and assess the damage that such an event would cause. This is done through one of a few currently relevant methods: (1) qualitative assessment, which offers a broad overview of risk but lacks detail, (2) mechanistic modeling, which can provide detailed results but requires detailed knowledge or assumptions about the tree composition, or (3) empirical modeling, which aims to provide a compromise between accuracy and ease of calculation.

Several models have been designed to assess the risk posed to trees by wind. The three most widely used and referenced are HWIND (van Schooten, 1985), a mechanistic model that integrates regional wind profiles and the SIMA ecosystem model (Kellomäki et al., 1992) to assess risk for forest stands. ForestGALES (Gardiner and Quine, 2000) integrates soil characteristics and GIS data to improve estimates of overturning risk compared to HWIND. Lastly, FOREOLE (Ancelin et al., 2004) employs a mechanical model to better represent the risk of trunk rupture, and is capable of evaluating heterogeneous forest stands with different tree species and ages of trees. All three models simulate forest stands and cannot assess wind risks to a single tree. These models also all exclusively consider coniferous trees, and none account for how the aerodynamic properties of trees may be affected by changing climatic conditions.

In this study, we propose a model to address these limitations by simulating anthropogenic climate change effects on a lone silver birch (*Betula pendula*) tree grown in Toronto, Canada. Specifically, atmospheric CO_2 concentrations are rising at an unprecedented rate (N. US Department of Commerce). Higher CO_2 concentrations result in larger, faster-growing trees (Curtis and Wang, 1998). It is predicted that this will increase trees' risk to damage in wind storms, as their larger size will increase the drag force they face from the wind. This shift in tree growth and potential shifts in allometry are not currently represented in wind tree damage models, but can have significant impacts on both the likelihood of a tree being damaged by wind, as well as the cost to repair the damage. As trees grow larger, they experience larger drag forces from the wind. Larger trees have greater wind-facing area to be impacted by the wind. Taller trees have a higher center of pressure,

* Corresponding author at: Western University, 1151 Richmond St, London, ON N6A 3K7, Canada.
E-mail address: swoolse2@uwo.ca (S. Woolsey).

https://doi.org/10.1016/j.agrformet.2023.109732
Received 17 January 2023; Received in revised form 18 August 2023; Accepted 22 September 2023
Available online 27 September 2023
0168-1923/© 2023 Elsevier B.V. All rights reserved.

creating a larger base bending moment. Trees with greater leaf area have more surface area, and either increased crown volume, crown density, or some combination of both of these changes which will increase the drag force experienced by the tree from the wind. The frequency and intensity of windstorms is also changing as the climate warms: both mean and maximum wind speeds have increased in the past 40 years in the Toronto region (Romanic et al., 2018). It is predicted that the increase in maximum wind speeds observed will increase trees' risk to damage in windstorms since the storms are increasing in intensity, subsequently increasing the drag force applied on trees from the wind. These underrepresented factors are implemented into our modeling to determine how they affect the return period of tree failure events through overturning or trunk rupture, and what cities can do to better mitigate this risk. The proposed methodology will assess the risk of a 30-year-old silver birch tree failing via overturning or trunk rupture from wind for atmospheric CO_2 and wind conditions local to Toronto from 1990, 2020, 2050 and 2080.

Silver birch was selected as the test species for the model because a concurrent experiment was conducted at Western University's Biotron Experimental Climate Change Research Centre, where paper birch (*Betula papyrifera*) trees were grown with an ambient CO_2 treatment (AC, 450 ppm), and an elevated CO_2 treatment (EC, 750 ppm), to collect data that are used in our model. Silver birch and paper birch are closely related tree species, having a similar mature size and structure, as well as similar leaves. Since some areas of the proposed model were lacking data, these two experiments were conducted together to improve the model by providing additional first-hand data with which to validate the model results.intre Trees of the genus *Betula* account for 1.6% of trees, and 3 % of total leaf area in the city of Toronto as of 2013 (City of Toronto, 2013).

The objective of this study is to propose a method for estimating the return period of a failure event for a tree due to windstorms, and how this return period will change due to climate change as the concentration of CO_2 in the atmosphere is rising at an unprecedented rate, and windstorms are possibly changing in both frequency and intensity globally. The proposed method is broadly applicable to any tree where data are available about the size, shape and strength of the tree at maturity. To show how the method can be applied in practice, results are presented for an average silver birch tree (*Betula pendula*). The physical and aerodynamic properties of the tree, and the changes the tree would experience in future CO_2 conditions, will be estimated from the literature and supplemented with experimental data.

The model works by first estimating the size and shape of the tree in current CO_2 concentrations. Then, we estimate how the tree's size and shape would change with different concentrations of atmospheric CO_2 in the past and in the future. Once the tree traits are defined, we calculate what drag force is required to cause tree failure (through trunk rupture or overturning). We find the wind speed required to create this drag force, and what the likelihood of that wind speed being reached or exceeded annually is, both under current conditions and by projecting wind speed trends into the future.

2. Model methodology

2.1. Defining tree size and shape

The size and shape of the silver birch tree was estimated using the United States Department of Agriculture (USDA)'s Urban Tree Database of allometric equations (McPherson et al., 2016). This database is comprised of empirical relationships between different size parameters for 171 distinct tree species measured across the United States. 14,487 individual trees grown in urban environments were measured, and different types of functions were tested to relate each pair of parameters to determine the best fit. The USDA equations for silver birch are fitted to data from 29 trees grown and measured in the inland valleys climate zone, including Sacramento, Modesto, and Santa Monica, California. These cities have on average 8 °C warmer daily high temperatures during the growing season compared to Toronto, and similar night temperatures (Applequist et al., 2012). California also receives 0–5 mm of rainfall per month during the summer, while Toronto receives 60–80 mm of rainfall (Durre et al., 2013). Although these climates differ, the USDA database is the only large set of data where birch trees are observed into maturity, so the size and shape of the silver birch were estimated using these equations:

$$D = 2.53 + 0.880 \cdot age, \tag{1}$$

$$cdia = -1.41 + 0.885 \cdot D - 0.0338 \cdot D^2 + 0.00044 \cdot D^3, \tag{2}$$

$$chei = \exp(-0.532 + 2.38 \cdot \ln(\ln(D+1)) + 0.0730 \div 2)), \tag{3}$$

$$thei = \exp(0.168 + 1.93 \cdot \ln(\ln(D+1)) + 0.0365 \div 2)), \tag{4}$$

$$LA = \exp(0.195 + 3.92 \cdot \ln(\ln(D+1)) + 0.185 \div 2)), \tag{5}$$

where D is the diameter of the trunk at breast height [cm], age is the age of the tree [$years$], $cdia$ is the diameter of the crown [m], $chei$ is the crown height [m], $thei$ is the tree height [m], and LA is one-sided green leaf area [m^2]. All equations had r-squared values between 0.751 and 0.859, indicating a good fit to the measured data.

Fig. 1 shows a schematic drawing of the USDA tree size and shape dimensions, defined above in Eqs. (1)–(5). Additionally, the perpendicular distance from the soil surface to the center of pressure of the crown, L, is defined and the location of the center of pressure, CoP, is shown. Due to lateral and longitudinal symmetry of the crown, the center of pressure is located at the centroid of the crown when viewed from the front. From the top view looking down upon the tree, the covered ground area, A_{ground}, is shown as the total ground area covered by the tree crown from this perspective.

Some additional values that will be used in aerodynamic calculations were found using the geometry of the crown shape. Since a silver birch crown grown in open air closely resembles an ellipsoid, the crown was approximated as such (Fig. 1). The primary dimensions of the tree crown determined above from the USDA equations are used to determine the frontal area, A [m^2], and the covered ground area, A_{ground} [m^2], along with the leaf area index, LAI [m^2/m^2], and the volume of the crown, V_{crown} [m^3] using the following equations:

$$A = \pi \cdot \frac{cdia}{2} \cdot \frac{chei}{2}, \tag{6}$$

$$A_{ground} = \pi \cdot \left(\frac{cdia}{2}\right)^2, \tag{7}$$

$$LAI = \frac{LA}{A_{ground}}, \tag{8}$$

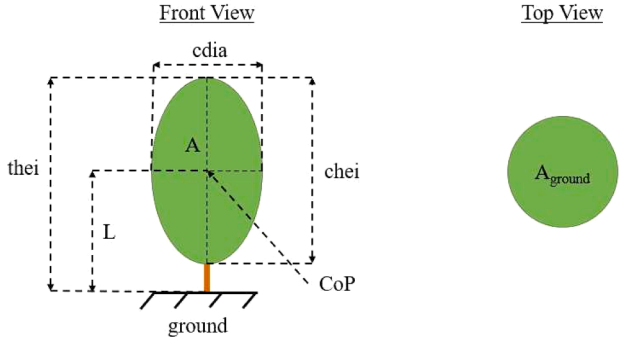

Fig. 1. Schematic drawing showing the dimensions of the silver birch tree that are used in the model.

$$V_{crown} = \frac{4}{3} \cdot \left(\frac{cdia}{2}\right)^2 \cdot \frac{chei}{2}, \quad (9)$$

2.2. Estimating the impact of elevated CO_2 concentrations on tree growth parameters

The effects of climate change were simulated at 30-year intervals for a silver birch tree for 1990, 2020, 2050 and 2080. Atmospheric CO_2 concentration data are available from March 1958 from the Mauna Loa observatory in Hawaii, USA, (N. US Department of Commerce, 2023). By beginning the analysis in 1990, more than 30 years of data were available to train the model.

To investigate how elevated atmospheric CO_2 concentrations affect tree growth and tree resilience to high wind speeds, the Web of Science database (Clarivate, 2022) was searched for studies that imposed an elevated atmospheric CO_2 treatment on trees, with all other factors kept constant, and then measured at least one of the variables of interest, shown below in Table 1.

To be included in the meta-analysis, papers must have listed the CO_2 concentrations used, the tree species, the sample size, the duration of growth, and the age of the trees used. Individual observations were required to be statistically independent, so only one measurement point per treatment per study was used. In total, 766 papers were found using these search terms. From these criteria, 219 papers were collected, encompassing 293 tree samples. 23 variables were measured across these studies, eight of which will be used in this study: total biomass, root biomass, leaf biomass, stem biomass, total leaf area, stem height, stem diameter, and stem density. Data presented in tables in the studies were taken directly, while data presented in figures were extracted from graphs using DataThief III (2022).

Changes in tree parameters that affect how much force a tree can withstand from wind were calculated by adjusting the tree parameter values using the mean results of the meta-analysis. We assumed that the variables of interest change linearly between the control CO_2 concentration (~365 ppm) and the elevated CO_2 concentration (~700 ppm). A limited amount of data was available to model how gradual increases in CO_2 concentration will affect tree growth, as 248 out of the 293 tree samples studied were grown under elevated CO_2 concentrations greater than the predicted 2080 level used in the model. A linear relationship was selected since no clear trend was present from the remaining 45 tree sample data. Since the USDA allometric equations are made from empirical data of current trees, tree properties for the current (1990–2020) period are solved for directly from Equations 1 - 5. From the meta-analysis results, we observed what mean percentage change each tree property shows when the growth CO_2 concentration is increased by 335 ppm (from 365 ppm to 700 ppm CO_2). Using the current period tree properties as a reference, our model scales the meta-analysis results by the change in CO_2 concentration between the current period and the other three periods using the following linear equation;

$$Var(X) = Var(USDA) \cdot \frac{CO_2(X) - CO_2(2020)}{CO_2(elevated) - CO_2(control)} \cdot Var, \quad (10)$$

where $Var(X)$ is the value of the relevant tree parameter in year X, $Var(USDA)$ is the value of the relevant tree parameter obtained from Eqs. (1)–(5), $CO_2(X)$ is the CO_2 concentration in year X, $CO_2(2020)$ is the mean atmospheric CO_2 concentration from the 1990–2020 period, $CO_2(elevated)$ is the mean elevated CO_2 concentration used in the meta-analysis studies, $CO_2(control)$ is the mean control CO_2 concentration used in the meta-analysis studies, and ΔVar is the mean observed change of the tree parameter from the meta-analysis.

Each tree parameter calculated using this method was also analyzed for sensitivity on the final results of the model. Each parameter was calculated with the mean observed change, ΔVar, and with the mean value $\pm$ 1 standard deviation. Simulations were run with the variance data to maximize their impact on the fragility of the tree. To compute the maximum fragility of the tree, parameters that were shown to increase fragility as they rose would incur $a + 1$ standard deviation change, while parameters that were shown to decrease fragility as they rose would incur a -1 standard deviation change. To compute the minimum fragility of the tree, the opposite relationships were applied.

The CO_2 concentrations used for the 1960–1990 and 1990–2020 time periods were extracted from atmospheric CO_2 data measured at the Mauna Loa observatory (N. US Department of Commerce, 2023). To predict CO_2 concentrations for the 2020–2050 and 20,502,080 periods, we used the Intergovernmental Panel on Climate Change's (IPCC's) RCP8.5 emissions scenario CO_2 prediction data (IPCC, 2014). The IPCC produced four representative concentration pathways (RCPs) as part of their Fifth Assessment Report, which are used for making projections of climate change based on different 21st century pathways of anthropogenic activity. The RCP8.5 scenario was selected because it includes the highest level of atmospheric CO_2 increase, which has most closely resembled the real atmospheric CO_2 concentration trajectory since the four RCPs were published in 2014.

2.3. Estimating tree strength

Critical loads to overturn or rupture the modeled tree were calculated, and the lower of the two loads was considered the critical load that will cause failure.

The force required to overturn the tree was calculated using an empirical function, based on tree pulling experiments. These tests, by van Schooten (1985) and further analyzed by Peltola (2006), involved loading 11 birch, 33 spruce, and 51 pine trees with a winch attached 6 m from the ground around their stems, and measuring the bending moment at the tree base required to overturn the trees. The base bending moment values were recorded along with the diameter at breast height (D) of each tree, and a function of the following form was fitted to the data. From the empirical overturning function, the best fitting function for mature birch trees is (Peltola, 2006):

$$F_{overturn} = \frac{66.2 \cdot (D \div 100)^{2.07}}{L}, \quad (11)$$

where $F_{overturn}$ is the force required to overturn the tree [N], D is tree trunk diameter at breast height [m], and L is perpendicular distance from the soil surface to the center of pressure of the crown. The center of pressure is shown in Fig. 1, where, due to lateral and longitudinal symmetry of the crown, it lies along the axis passing through the center of the crown.

The trunk of a tree will rupture when the shear stress within the trunk exceeds the modulus of rupture. To calculate shear stress within the trunk, the tree is approximated as a cylindrical cantilever beam, where it is fixed to the ground by its roots and is free to move at the crown. The force that can be supported is found based on the equation for the maximum bending stress within a cantilever beam fixed in this

Table 1
Elevated CO_2 concentrations increase the growth of trees. Percent changes in growth parameters for trees grown under elevated CO_2 levels (540–800 ppm) compared to control CO_2 concentrations (320–460 ppm), shown as mean values $\pm$ standard deviations.

Variable studied	Number of studies	% Change
Total Mass	194	42.8 ± 49 %
Root Mass	143	48.3 ± 44 %
Leaf Mass	134	42.8 ± 58 %
Stem Mass	123	46.9 ± 51 %
Leaf Area	102	29.1 ± 32 %
Stem Height	113	20.7 ± 27 %
Stem Diameter	52	15.4 ± 12 %
Stem Density	9	0.4 ± 5.8 %

way:

$$F_{rupture} = \frac{\pi \cdot (D \div 100)^3 \cdot MoR}{32 \cdot L}, \quad (12)$$

where $F_{rupture}$ is the force required to rupture the tree trunk [N], and MoR is modulus of rupture of the tree trunk [Pa] which is used in place of maximum bending shear stress, $\sigma_{bend,\max}$.

The USDA reports the modulus of rupture for silver birch trees to be 57 MPa (Green et al., 1999). In the model, values of 85 % of the modulus of rupture derived from static tests on clear samples of green wood were used, based on data for birch that suffered stem breakage during tree pulling experiments (Kellomäki and Peltola, 1998). This correction is made to account for the presence of knots and other wood imperfections which are present in naturally grown trees but are avoided in mechanical properties reference manuals.

Due to the non-conclusive data found in the meta-analysis regarding the relationship between CO_2, tree growth, and modulus of rupture, no assumption was made about changing modulus of rupture with each time period. This is an aspect of wind damage modeling that would benefit from future work to better define the load capacity of the simulated tree for trunk rupture failure.

2.4. Estimating damaging wind speed

The wind speed required to create a critical drag force is found based on the drag equation;

$$V = \sqrt{\frac{2 \cdot F}{\rho \cdot A \cdot C_D}}, \quad (13)$$

where V is wind speed [m/s], F is drag force [N], ρ is air density [kg/m^3], A is crown frontal area [m^2], and C_D is a non-dimensional drag coefficient.

An important note to make is that the drag coefficient of a flexible object, like a tree crown, is not constant with wind speed. The tree crown expands as the forward branches are bent perpendicular to the wind at low wind speeds and then streamlines at higher wind speeds, as recently described by Enuş et al. (2020). The extent to which a tree crown can be reconfigured varies between species, and between trees of the same species due to variations in crown shape, leaf size and shape, branch stiffness, crown density, and other factors that impact the flexibility and aerodynamics of the tree. Mayhead (1973) reported an example of this, where Pinus trees ranged in drag coefficient from 0.3 to 0.45 at 9 m/s wind speed, and from 0.2 to 0.3 at 25 m/s wind speed. The drag coefficient of a tree decreases as wind speed increases since the tree leaves and branches are reconfigured and streamlined by the wind. At lower speeds, Enuş et al. (2020) reported a 27 % decrease in drag coefficient when wind speed is varied from 1.4 to 6.3 m/s. Experimentally, Mayhead (1973) found that silver birch trees tested at the maximum wind speed they could withstand before being damaged had a drag coefficient of 0.29, the value used in this work as the baseline value for the modeled tree.

2.5. Estimating damaging wind speed return period

To determine the likelihood of the critical wind speed being exceeded annually, historical wind gust data from Toronto Pearson International Airport, were analyzed. Daily maximum 3–5 s wind gust data are available from January 1957, providing the longest available record of wind data in the region. The data were filtered to consider only days from April to October, when trees are likely to have their full foliage in Toronto. A Weibull distribution was created of the annual maximum wind gust speeds using linear regression to show the historical probability of a given wind speed being exceeded in any year with recorded data.

A Weibull distribution is a continuous probability distribution that is frequently used in the field of wind engineering, due in part to its simple form and high flexibility. This model uses the cumulative distribution function (CDF) form of the Weibull distribution to estimate the likelihood of a given wind speed being reached or exceeded on a specified interval. The fitted Weibull CDF has the following form:

$$P_{exc} = \exp\left(-(V \cdot c)^K\right) \quad (14)$$

where P_{exc} is the probability that the gust wind speed, V, will be exceeded during an interval, c is the unitless scale parameter, and K is the unitless shape parameter of the distribution.

The return period, T, of a certain gust wind speed is found as the reciprocal of the probability of exceedance:

$$T = 1 \div P_{exc}, \quad (15)$$

To investigate how peak wind speeds have changed over time, the Pearson Airport daily maximum wind gust data were divided into two periods: 1960–1990 and 1990–2020. A Weibull distribution was fitted to the entire data set using linear regression (Fig. 2). A Weibull distribution was then fitted to the data from each 30-year period, and the two 30-year data sets were compared against each other (Fig. 3). A student's t-test was performed between the two 30-year periods of data to quantify the significance of trends in the data. To evaluate any trends in wind climatology over wider region, broader papers were referenced. Romanic et al. studied wind trends in the greater Toronto area (Romanic et al., 2018), and the IPCC studied wind trends in northern-mid latitudes (Seneviratne et al., 2012) and across all latitudes (Hartmann et al., 2013).

3. Results

3.1. Tree size, shape and strength

The meta-analysis results are integrated in the tree growth model as follows: (1) leaf mass changes the crown volume, V_{crown}; (2) stem height changes tree height, $thei$; (3) stem diameter changes diameter at breast height, D. Data on how elevated CO_2 conditions alter stem density, the modulus of rupture, and the modulus of elasticity were also sought in the meta-analysis, but little information was found about the impact of elevated CO_2 on these variables, so no CO_2 effect on these parameters was assumed in the model. The CO_2 concentrations used in the model for the 1960–1990 and 1990–2020 periods were 332 and 380 ppm, respectively. These values were taken directly from the Mauna Loa observatory data. For the 2020–2050 and 2050–2080 periods, the concentrations used were 475 and 644 ppm, respectively. These values were extrapolated using the IPCC's RCP8.5 emissions scenario (IPCC, 2014).

The above table of tree sizes was generated using the effects of elevated CO_2 on tree growth meta-analysis, which showed the following mean results. The relevant variables studied, and their results are summarized below.

Trees are 43% heavier when subjected to elevated CO_2 treatments compared to ambient CO_2.

The variance in each variable in Table 1 is high, owing to the wide variety of tree species, study duration, elevated and control CO_2 concentrations included in the meta-analysis. Of the 183 tree samples collected, 28 were birch (*Betula* spp.), five of which were silver birch (*Betula pendula*). The meta-analysis data was also analyzed after filtering only for birch, and again after filtering only for silver birch. Both of these filtering processes did not significantly improve the quality of the data, as the birch results still had large variances in the same order as the full data set, and the silver birch results were limited to a sample size of five studies, reducing their significance. Due to the high variance, only the mean values from the meta-analysis data were used to define tree growth parameters for each CO_2 level.

We estimated an average tree size and shape for a mature (30-year-

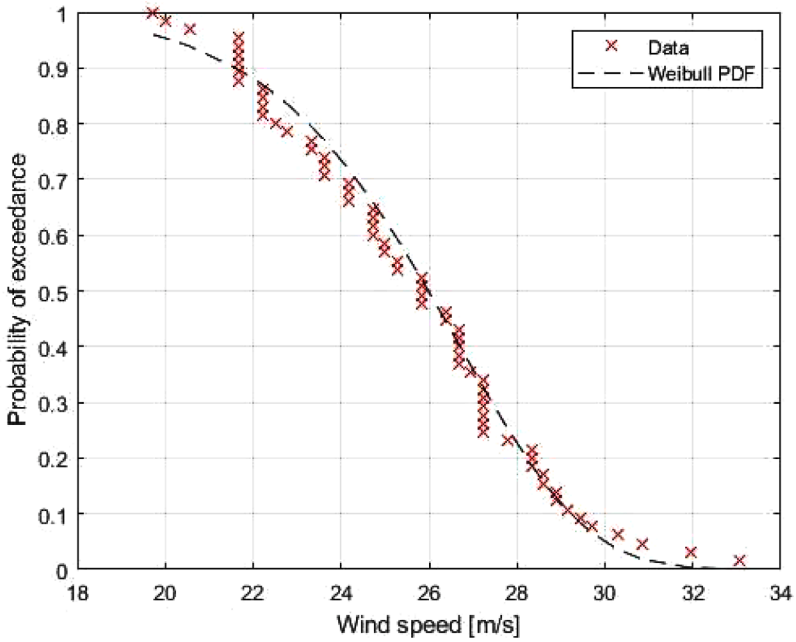

Fig. 2. Weibull cumulative distribution function of annual maximum wind speeds recorded at Toronto Pearson International Airport. Data is filtered to only include months from April to October 1957–2020.

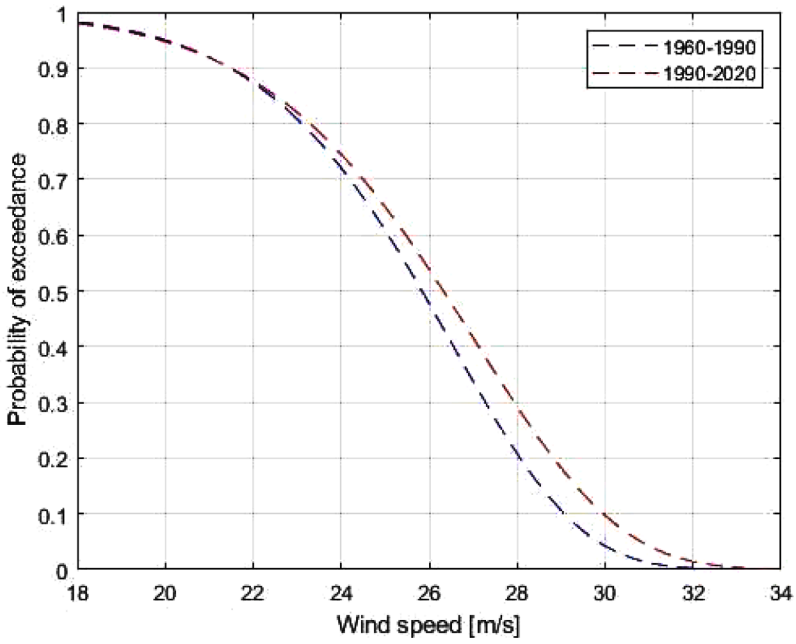

Fig. 3. Weibull cumulative distribution functions of annual maximum wind speeds recorded at Toronto Pearson International Airport. Data is filtered to only include months from April to October 1960–2020. Plotted in two 30-year intervals, 1960–1990 (blue) and 1990–2020 (red).

old) silver birch tree by first solving the USDA allometric equations for a tree grown under current conditions (year 2020) by inputting $age = 30$ into Eq. (1), then inputting the resulting trunk diameter at breast height (D) value into Eqs. (2)–(5). To determine the tree properties in the other periods of interest, the tree meta-analysis properties described in Table 1 are scaled for each time period using Eq. (10). The results of this interpolation of growth properties for each year of interest are summarized below.

The tree is larger under future growth CO_2 conditions, but not equally across all the parameters. The largest increase is seen in the crown frontal area, A, at a 27 % increase. The increasing trunk diameter, D, will improve the resistance of the tree to wind damage, while the increasing tree height, *thei*, and crown frontal area, A, will make the tree more vulnerable to wind gusts. The variance introduced by the meta-analysis data is most prevalent in the future tree conditions as the concentration of atmospheric CO_2 is expected to rise more rapidly than in the past. This has a relatively small impact on the trunk diameter, D, indicating that the load capacity of the tree, as defined in Eqs. (11) and (12) is unlikely to change substantially. The variance has a large impact on the perpendicular distance from the soil surface to the center of pressure of the crown, L, indicating that the base bending moment applied on the tree by the wind can change substantially due to variance.

Once all updates to the tree's size and shape were made, the model was run to determine the wind drag force required to damage the tree

via overturning ($F_{overturn}$, Eq. (11)) or trunk rupture ($F_{rupture}$, Eq. (12)). Whichever failure mode has a lower damaging drag force will be the critical failure mode, and the wind speed required to generate this damaging drag force (V, Eq. (13)) was determined. The results of this process are shown in Table 3.

Since the force required to overturn the tree is lower than the force required to rupture the tree trunk in all cases, overturning is the critical failure mode and is used to calculate the failure wind speed.

For both overturning and rupture, the force required to damage the tree is increasing in time and with CO_2 levels. The tree is getting a larger diameter and height at about the same rate, but the impact of larger diameter is much greater on the strength of the tree. The strength of the tree to overturning is proportional to $D^{2.07}$, and inversely proportional to tree height, from Schooten's empirical tree pulling test results that relate root strength to trunk diameter at breast height (van Schooten, 1985). The increase in trunk diameter has a much stronger positive effect on overturning strength compared to the negative effect of the tree growing taller at a similar rate. Similarly for trunk rupture, mechanically the maximum shear stress that the trunk can support is proportional to D^3, and inversely proportional to tree height. The elevated CO_2 growth conditions that will be present in the future will increase the force that trees can withstand.

Conversely, the wind speed required to damage the tree is shown to decrease as time advances. This is due to the increase of crown volume, and subsequently crown frontal area, A, as the crown diameter ($cdia$) and crown height ($chei$) are increased within the model Eqs. (9) and ((6)). This increases the drag force experienced by the tree for a given wind speed (Eq. (13)). As the crown frontal area increases by 27 % from the 1990 scenario to the 2080 scenario, the wind speed required to create a critical drag force is lowered by 6 % (1.9 m/s). Despite the silver birch tree being modeled to have a more resilient woody structure through increasing trunk diameter, it will become more fragile due to the growing crown size and trunk height.

Uncertainty in these results introduced by the meta-analysis data variance is greatest in the future tree conditions as the concentration of CO_2 is expected to rise more rapidly than in the past. By 2080, the maximum overturning and rupture forces, and critical wind speeds are all more than twice their minimum bounds. This is a very high variance, owing to the wide variety of data that had to be included in the meta-analysis to produce a large enough data set.

3.2. Wind speed return periods

The model concludes by estimating the likelihood that the critical wind speeds, V, found above, are met or exceeded annually. To do this, the Toronto Pearson Airport data set of annual maximum wind speeds from April to October is fitted by a Weibull distribution. This is shown in Fig. 2, where the maximum wind speed recorded at the airport in each year is plotted in ascending order, alongside the fitted Weibull cumulative distribution function.

Each red X in the figure represents the highest 5 s sustained wind gust that was recorded in a given year from 1957 to 2020, during April to October period. These annual maximum gusts are plotted in order from lowest to highest, against annual probability of exceedance. The probability of exceedance is calculated as the likelihood that a certain wind speed will be given in any given year between 1957 and 2020, where the lowest wind speed will have a 64-in-64 chance of occurrence, and the highest wind speed will have a 1-in-64 chance of occurrence. The Weibull distribution is fitted to this data via linear regression, shown as the black hashed line. The fitted probability of exceedance function has the following expression;

$$P_{exc} = \exp\left(-(V \cdot 0.037)^{10.22}\right), \tag{16}$$

where P_{exc} is the probability that a given wind speed occurs annually, and V is wind speed [m/s].

The fitted Weibull has an r-squared value of 0.95, indicating a good fit to the data.

To test whether the wind gust data is consistent between all 64 years in the period, with the same mean and standard deviation, or if these probability factors are changing, the data was divided into 2 sets. The first 30 years, 1960–1990, was plotted, alongside the next 30 years, 1990–2020. These subsets were each fitted with Weibull CDFs following the same linear regression procedure used to fit the full data set. The resulting Weibull CDFs of the two 30-year sets of data are shown below in Fig. 3.

These two periods appear to be quite different, particularly in the 28–31 m/s wind speed range, where our model shows most trees will be critically damaged, and these winds occur about twice as often in the 1990–2020 period compared to the 1960–1990 period. However, a student's t-test was performed to compare the two 30-year periods of data, and no difference was found at the 5% significance level ($p = 0.5$), making it likely that the apparent increase in frequency of high wind speeds in the 1990–2020 data compared to the 1960–1990 data is due to random chance. Additional analysis on global and local wind trends was conducted by reviewing literature to validate the results found from the Toronto Airport data.

Limited data are available to model how the intensity and frequency of windstorms are affected by climate change. Specific to Toronto, Romanic et al. reported a mean wind speed increase of 0.2 m/s over the period from 1948 to 2014 (Romanic et al., 2018). This increase was observed primarily during the fall and winter seasons, when wind speed increased 0.54 m/s. In contrast, spring and summer showed "almost negligible and statistically not significant trends" in wind speed over this same period (Romanic et al., 2018). Due to the low confidence of these findings, the return periods of high wind speeds were therefore not changed in the model. In a global analysis of changes in climate extremes produced in the Fifth Assessment Report by the IPCC, changes in observed surface winds over land across all latitudes were assigned a low confidence level (Hartmann et al., 2013). The IPCC also published a special report on managing the risks of extreme events and disasters (SREX), wherein a strong decline in extreme winds compared to mean winds was reported for the continental northern-mid latitudes (Seneviratne et al., 2012). This result was also assigned a low confidence level. Overall, the data currently available is limited in quality (due to inconsistencies between measuring techniques at different sites), quantity (due to relatively short time spans of data collection), and spatially (where most measuring sites are close to urban centers).

Once all updates to the model are made as described in Sections 4.1 and 4.2, above, the following results were found. The tree size, shape and strength are changed as described in Tables 2 and 3, and no changes are made to the wind speeds for either frequency or intensity due to the aforementioned low confidence in available data. For each 30-year period ending in the years listed below in Table 4, the critical wind speed to damage the 30-year-old birch tree is listed, along with the probability that wind speed is exceeded annually, and the estimated return period of a damaging windstorm event.

Model predictions for the force required to damage a 30-year-old

Table 2
Model predictions for a 30-year-old silver birch tree's height, trunk diameter, leaf area, and perpendicular distance from the soil surface to the center of pressure of the crown. Predictions are made for the tree's properties in 2020 based on empirical growth models, and varied for the years 1990, 2050, and 2080 based on meta-analysis data studying the impact of increasing atmospheric CO_2 concentration on tree growth. Mean values are reported, ± 1 standard deviation introduced by variance in the meta-analysis data.

Year	thei [m]	D [cm]	A [m^2]	L [m]
1990	12.35 ± 0.59	28.24 ± 0.53	54.67 ± 2.24	6.95 ± 0.48
2020	12.68	28.92	56.86	7.17
2050	13.34 ± 1.18	30.27 ± 1.05	61.34 ± 4.90	7.61 ± 0.96
2080	14.50 ± 3.28	32.67 ± 2.92	69.73 ± 14.94	8.40 ± 2.65

Table 3
Model predictions for the force required to damage a 30-year-old silver birch tree via overturning or trunk rupture, and the wind speed required to generate the critical (lower) force in each year. Predictions are made for the year 2020 based on empirical growth models, and varied for the years 1990, 2050, and 2080 based on meta-analysis data studying the impact of increasing atmospheric CO_2 concentration on tree growth. Mean values are reported, with minimum and maximum values within 1 standard deviation introduced by variance in the meta-analysis data in square brackets.

Year	$F_{overturn}$ [N]	$F_{rupture}$ [N]	V [m/s]
1990	9600 [8850; 10,700]	12,900 [11,730; 14,690]	31.4 [29.4; 33.9]
2020	9770	13,500	31.1
2050	10,100 [8350; 11,780]	14,500 [11,620; 17,480]	30.5 [26.6; 34.7]
2080	10,700 [6720; 15,960]	16,600 [9510; 26,690]	29.5 [21.1; 41.6]

Table 4
Model predictions for the wind speed, V, required to damage a 30-year-old silver birch tree via overturning, the critical failure mode. For each critical wind speed, the estimated probability of exceedance, P_{exc} is shown and the return period, T. Predictions are made for the year 2020 based on empirical growth models, and varied for the years 1990, 2050, and 2080 based on meta-analysis data studying the impact of increasing atmospheric CO_2 concentration on tree growth. Mean values are reported, with minimum and maximum values within 1 standard deviation introduced by variance in the meta-analysis data in square brackets.

Year	V [m/s]	P_{exc} [%]	T [$years$]
1990	31.4 [29.4; 33.9]	0.78 [8.5; 2.8e-03]	128 [11.8; 357]
2020	31.1	1.3	77
2050	30.5 [26.6; 34.7]	2.9 [41.49; 1.6e-04]	34 [2.41; 6.3e06]
2080	29.5 [21.1; 41.6]	8.3 [92.1; 1.1e-35]	12 [1.1; 9.1e34]

silver birch tree via overturning or trunk rupture, and the wind speed required to generate the critical (lower) force in each year. Predictions are made for the years 1990, 2020, 2050, and 2080 based on meta-analysis data studying the impact of increasing atmospheric CO_2 concentration on tree growth are presented.

Our model indicates that the critical wind speed to damage the silver birch trees will be steadily declining, with more drastic changes happening as time advances. Although the mean wind speeds are only declining by about 2 m/s across the entire interval, this results in a massive increase in the frequency of damaging storms occurring. Reviewing the Toronto Pearson data, the highest critical wind speed, 31.1 m/s, was exceeded twice in 64 years, while the lowest critical wind speed predicted for 2080, 29.5 m/s, was exceeded five times. Despite these wind speeds being separated by only 1.6 m/s, The fitted Weibull indicates that the lower critical wind speed is about ten times as likely to occur as the higher critical wind speed.

The variance introduced by the meta-analysis data has propagated through the damaging wind speed, V, values such that the calculations of maximum and minimum probabilities of exceedance and their respective return periods are impractical. Since the maximum wind speed observed in the Toronto Pearson data was 33 m/s throughout the 64 year period on record, it is impractical to use the fitted Weibull distribution to estimate the likelihood of any of the upper bounding wind speeds from occurring in the region.

4. Discussion

4.1. Modelling results

Based on what is known about how elevated concentrations of atmospheric CO_2 impact tree growth, the slightly lower critical wind speed for failure of the simulated silver birch tree as time advances seems reasonable. Low confidence is assigned to the more than ten times greater probability of failure though, which is too drastic. This is due to the limited data available to predict these inherently rare high wind events, and to assess what impact climate change is having on local and global winds. In Fig. 2, the 1957–2020 data indicates very few events registered for the wind speeds greater than 29 m/s. Since all available data currently indicates a low confidence in any significant changes to windstorms frequency or intensity, both locally in Toronto as well as globally, the model cannot accurately predict this. The wind gust data at Toronto Airport were selected due to the long duration of observations available (since January 1957), given that there are no similar records available from within the city. The airport data were selected as they were the longest record available in the region, which was essential to improve confidence in the wind trend observations.

Our model indicates that the mean CO2 concentration in 2050–2080, the period with the highest CO2 concentration, will be approximately 545 ppm. Only 35 out of 293 studies included in the meta-analysis had elevated CO2 concentrations less than 600 ppm, and none used elevated CO2 concentrations less than 540 ppm. Due to the lack of intermediate CO2 study data that can be directly applied to estimate the tree properties in the test period 19,902,080, a linear change is assumed as there is no clear trend present in the remaining available data. This categorical approach is similar to previous meta-analyses of elevated CO2 effects on plant growth and physiology (Ainsworth and Long, 2004; Poorter and Navas, 2003).

Table 1, showing the increases in each growth parameter due to elevated CO_2 concentration, indicates that on average slightly more tree mass is concentrated in the roots compared to the leaves and stem. This indicates that tree resilience to overturning should improve by lowering the center of mass. This allometric shift is not reflected in our current tree wind resilience model though, since how the strength provided by the roots of a mature tree will change with different root sizes and orientations is not well understood. Current wind damage models circumvent this by using empirical relationships from tree pulling experiments to relate the force required to overturn a tree, and the trunk diameter at breast height (van Schooten, 1985). The variance on meta-analysis variables reported on in Table 1 have high variance. This could be improved in future by increasing the data set size most relevant to the specific tree being examined in age, species, and climate.

Despite the stated uncertainties, the results from this model are significant because they indicate a trend of increasing fragility for open-grown trees. Similar models could be constructed using different estimations, assumptions and data, but considering the comprehensive literature review and data meta-analysis that were conducted with the creation of this model, we are confident that the same trend will be found. The model showcases wind risk for trees from a climate change perspective, which is growing in importance as global environmental conditions continue to change at an unprecedented rate. Atmospheric CO_2 is rising and will continue to do so, along with many other factors related to tree's risk, such as storm intensities and frequencies, and temperature rise. It is more important now than ever before to consider the effects that such changes will have on trees' strength and resilience so that appropriate action can be taken to mitigate these rising risks.

4.2. Comparison to other wind damage and climate models

The present model is a first to estimate how climate change will affect the fragility of trees. Other models, where the growth parameters of trees can be varied, have focused only on current climate conditions. Also, our model is more broadly applicable for any tree species, since we have collected up-to-date information about the growth parameters and impact of elevated CO_2 on a wide range of species. The model is also modular, where the tree strength and wind calculations can be easily adjusted as more precise data becomes available in future about how trees are impacted by climate change.

The results of other models are not directly comparable to the model developed here due to the different species tested and their respective strength properties. As a general indicator of our model's performance, we recorded that Gardiner and Quine predicted that a 30-year-old stand

of Sitka spruce trees would fail at 30.5 m/s via overturning in current climate conditions using the ForestGALES model (Gardiner and Quine, 2000).

For the meta-analysis data collected, our results indicate slightly higher growth in the elevated CO_2 treatment compared to Curtis and Wang's 1997 meta-analysis on woody plant mass. They found mean increases of 29 % total biomass, 37 % leaf biomass, and 38 % stem biomass (Curtis and Wang, 1998). For the purpose of this model, a new meta-analysis was completed instead of using a previous review paper because of our desire to further filter the data. When constructing the model, consideration has been given to how many data points were available that were more specific to the example problem of a 30-year--old silver birch tree than a general meta-analysis of all trees. Data from 5 studies that included silver birch (*Betula pendula*), and 28 that included birch (*Betula* spp.) was considered.

4.3. Designing the model

When integrating the meta-analysis results into the model, it was challenging to find growth parameters that are directly measured in typical elevated CO_2 growth studies and that relate directly to a tree's resilience to wind damage. Most of these studies are conducted from a purely biological perspective, measuring photosynthesis and respiration related chemical properties within the trees, along with high-level tree size variables. Due to this, estimations had to be made about how to integrate leaf area, leaf mass, root mass, crown drag coefficient, and stem density that would be impactful to the model and are supported by literature. Due to the lacking available information in literature, many of these factors could not be considered in the model. This is an aspect of the model that could be greatly improved in the future with more targeted studies to begin to answer these unknowns.

The wind damage model of equations proposed in this paper were selected based on their suitability for modeling leafy trees, as well as for the ability to adjust the physical properties of trees that change with elevated CO_2. The USDA allometric relationship equations were selected to define the silver birch size and shape because the USDA urban tree database provides a wide range of tree species that have good sample sizes and include trees of a wide range of ages. Additionally, to estimate risk for other tree species, the USDA database has a wide range of tree species that can be easily referenced to update the model. The calculation of overturning resistance by following Schooten's empirical D equation, and rupture force via the mechanical shear stress equation is a standard practice, found in other wind damage models. Tree pulling experiments do not necessarily represent the same loads as high wind speeds on trees with respect to these failure modes, but testing mature trees at critical wind speeds greater than 30 m/s is highly impractical due to the combination of facility and wind scales. Due to this, such work has not been undertaken by any researchers to date.

To calculate the drag force applied on the tree by the wind, multiple models were considered before the classical drag equation was selected. Other options included the Darcy-Forchheimer equation for flow through a porous medium, which has been used by Koch et al. (2019) to characterize the flow of air through tree branches, but not enough information about the porosity of the crown of a tree was available in open air to make this feasible. A more detailed mechanistic model for the tree crown was also considered, but too many assumptions about the tree branches, leaves and their interaction with the oncoming air were required to produce confident results for the average tree. The classical drag equation was selected because it offered a good compromise between model resolution and ease of calculation. The air density ρ, wind speed V, and crown area A, can all be easily assumed, calculated or measured. The main source of variability in this type of model appears in the drag coefficient term C_D. In general, there is limited data available about the drag coefficient of different trees and their crowns, but the available studies quantify this relationship between the wind speed and drag force via the non-dimensional drag coefficient (Mayhead, 1973; Kane and Smiley, 2006; Kitagawa et al., 2015). The drag coefficient is the simplest method to account for the changing aerodynamic performance of a tree when climate change factors are considered in this model but its evolution with wind speed while somewhat addressed at low speeds (Enuş et al., 2020) needs further investigation for higher wind speeds.

When estimating the likelihood of a given wind speed being exceeded annually, the Weibull continuous probability distribution was used as it is the standard for wind engineering applications. The created function is used to estimate probability of exceedance for a given wind speed input simply and effectively.

Tree failures during winter were not considered for this study as the primary loads that cause failure during winter months are due to freezing, which stiffens the trees, making them brittle, and loading due to snow and ice weighing on the trees. These failure modes are beyond the scope of this study as these loads are applied differently than wind loads, and the tree growth parameters that change trees' risk to wind damage will not necessarily change their risk to winter loads. During months in which broadleaf trees are expected to be foliated, the primary failure modes are overturning and rupture, which were the modes evaluated. The higher wind speeds found in the months where the tree is expected to have lost its leaves are not likely to cause failure since the greatly increased porosity of trees without their leaves reduces the wind load on them very significantly.

Of the many climactic variables changing due to anthropogenic activity, atmospheric carbon dioxide concentration was selected for this study because it is shown to have a measurable, and substantial change on the growth of trees (Curtis and Wang, 1998). With the goal of integrating a climate change factor with a wind damage model in mind, it was essential to select a variable that had a wide range of data available to properly quantify the effects on tree growth. However, other variables impact this growth, such as the availability of other essential nutrients, like nitrogen (Yan et al., 2019), and need to be considered in future studies. Another climactic variable that is changing significantly due to anthropogenic activity is air temperature. Rising air temperatures are shown to typically suppress growth, but can have mixed effects depending on the specific region and plant species (Wang et al., 2012). To model rising temperatures, specific data would need to be collected about the species being modeled, along with the region's typical air temperature and trends with climate change. As global temperatures increase, the frequency and intensity of droughts are likely to rise as well (Seneviratne et al., 2012) which will change the growth response of local vegetation significantly.

4.4. Suggestions to improve future modelling

To improve confidence in the results, or to better understand the problem of climate change and trees' risk to wind damage, future work can improve upon some areas of this modeling that are currently poorly understood. Specifically, the modeled tree is much more likely to fail via overturning instead of trunk rupture, indicating that the tree is weakest due to its roots. The root model used in this study was based on van Schooten (1985) results, which only include a small sample of trees. In practice, it is difficult to get more detailed results beyond the work of Schooten, since the complex root systems of mature trees are not easily measured. This is an area of wind damage modeling as a whole that would benefit from further analysis, since the HWIND, ForestGALES, and FOREOLE models all use similar empirical functions to the one in this study. As well, as the leaf mass and area of the trees studied in elevated carbon dioxide indicate significant increases, an important area for model improvement is in the impact of these changes on the drag coefficient, C_D, of the tree crown. The results of the model are sensitive to any changes the aerodynamic performance of the tree crown, and only a limited number of studies have examined this topic. By conducting further tests to better understand how the drag coefficient of trees with more dense foliage will change, mostly at high wind speeds,

the confidence in this modeling technique can be improved significantly.

Due to the non-conclusive data found in the meta-analysis regarding the relationship between CO_2, tree growth, and modulus of rupture, no assumption was made about changing modulus of rupture with each time period. This is an aspect of wind damage modeling that would benefit from future work to better define the load capacity of the simulated tree for trunk rupture failure, since it is possible that with trees growing faster and larger due to rising CO_2, the strength of their trunk wood could change.

To reduce the high variance found in the meta-analysis results, further data filtering can be done to remove data from trees that are less relevant to the simulated tree. By only examining data of similar species, age, and climate conditions to those simulated, the confidence in growth trends will be improved. As the data set size is low, more research can be conducted specific to a desired combination of tree species, climate and age.

The meta-analysis is limited in practical application due to the optimal growing conditions that are provided to the trees. All the studies included had provided optimal water and nutrients to the trees, which is not reflected in the real world. This is likely to enhance the effects of the elevated CO_2 treatment beyond what will be present in reality as the trees are able to increase their growth rate more than if their growth was naturally limited by another source. As mentioned above, the only growth condition that was assessed in this study was elevated carbon dioxide concentration.

As the CO_2 concentration continues to rise in the atmosphere, our model indicates that silver birch trees will be at a greater risk of failure due to wind damage. Although the critical wind speed only decreases by about 2 m/s by 2080, this lower wind speed is about ten times as likely to occur. With the indication that trees will be more fragile to wind damage due to climate change, the importance of understanding and mitigating this risk has never been greater. To help protect trees in the future, urban planners can choose to plant tree species that have favourable properties to resist wind damage, like shorter and thicker trunks, thinner canopies, or stronger root networks to resist overturning. As well, arborists can trim trees to reduce excess foliage, and trim their tops to promote shorter growth to improve their resilience to wind damage (Kane and Smiley, 2006).

5. Conclusions

In summary, the synthesis of trees and wind with climate change to model the probability of failure to individual open-grown trees is a novel contribution to risk assessment of trees. The approach shown here is not widely used in other disciplines and is limited by a lack of empirical data for a few key parameters to become more robust, but is an effective starting point to better understand this problem. The risk of tree failure during windstorms will continue to increase in importance as we experience higher atmospheric carbon dioxide concentration and more damaging windstorms. With additional effort devoted to the modeling of more tree properties changing with high CO_2, or with other climate change related properties and their impact on trees such as temperature, or precipitation, this modeling technique could become a useful and practical tool for risk assessment of individual trees.

CRediT authorship contribution statement

Samuel Woolsey: Conceptualization, Methodology, Software, Validation, Formal analysis, Investigation, Data curation, Writing – original draft, Writing – review & editing, Visualization. **Horia Hangan:** Conceptualization, Methodology, Validation, Formal analysis, Resources, Writing – review & editing, Supervision, Project administration, Funding acquisition. **Hassan Peerhossaini:** Conceptualization, Methodology, Validation, Formal analysis, Writing – review & editing, Supervision, Project administration, Funding acquisition. **Danielle Way:** Conceptualization, Methodology, Validation, Formal analysis, Investigation, Resources, Writing – review & editing, Supervision, Project administration, Funding acquisition.

Declaration of Competing Interest

The authors declare the following financial interests/personal relationships which may be considered as potential competing interests: Samuel Woolsey has patent #Attribution-NonCommercial-ShareAlike 4.0 International (CC BY-NC-SA 4.0) licensed to Creative Commons license.

Data availability

Data will be made available on request.

Funding sources

This research did not receive any specific grant from funding agencies in the public, commercial or not-for-profit sectors.

References

Ainsworth, E.A., Long, S.P., 2004. What have we learned from 15 years of free-air CO_2 enrichment (face)? a meta-analytic review of the responses of photosynthesis, canopy properties and plant production to rising CO_2. New Phytol. 165 (2), 351–372. https://doi.org/10.1111/j.1469-8137.2004.01224.x.

Ancelin, P., Courbaud, B., Fourcaud, T., 2004. Development of an individual tree-based mechanical model to predict wind damage within forest stands. For. Ecol. Manag. 203, 101–121.

Applequist, S., Arguez, A., Durre, I., Squires, M.F., Vose, R.S., Yin, X., 2012. 1981–2010 us hourly normals. Bull. Am. Meteorol. Soc. 93 (11), 1637–1640.

Chiesura, A., 2004. The role of urban parks for the sustainable city. Landsc. Urban Plan. 68 (1), 129–138. https://doi.org/10.1016/j.landurbplan.2003.08.003.

City of Toronto, Parks, Forestry and Recreation, Urban Forestry, 2013. Sustaining & Expanding the Urban Forest: Toronto's Strategic Forest Management Plan. https://www.toronto.ca/data/parks/pdf/trees/sustaining-expanding-urban-forest-management-plan.pdf (accessed 4 August 2023).

Clarivate, 2022. Browse, Search, and explore journals indexed in the *Web of Science*. https://mjl.clarivate.com/home (accessed 18 March 2022).

Curtis, P.S., Wang, X., 1998. A meta-analysis of elevated co_2 effects on woody plant mass, form, and physiology. Oecologia 113, 299–313.

DataThief III, 2022. Welcome to Data Thief. https://www.datathief.org/ (accessed 18 March 2022).

Durre, I., Squires, M.F., Vose, R.S., Yin, X., Arguez, A., Applequist, S., 2013. Noaa's 1981–2010 us climate normals: monthly precipitation, snowfall, and snow depth. J. Appl. Meteorol. Climatol. 52 (11), 2377–2395.

Enuş, M., Dellwik, E., Mann, J., Hangan, H., Costache, A., 2020. Three-dimensional measurements of tree crown movement using an infrared time-of-flight camera. Exp. Fluids 61 (11), 1–13.

Gardiner, B.A., Quine, C.P., 2000. Management of forests to reduce the risk of abiotic damage ð a review with particular reference to the effects of strong winds. For. Ecol. Manag. 17.

Green, D.W., Winandy, J.E., Kretschmann, D.E., 1999. Mechanical Properties of Wood. In: Wood handbook—Wood as an engineering material. Gen. Tech. Rep. FPL–GTR–113. U.S. Department of Agriculture, Forest Service, Forest Products Laboratory, Madison, WI, p. 463.

Hartmann, D.L., Klein Tank, A.M.G., Rusticucci, M., Alexander, L.V., Brönnimann, S., Charabi, Y., Dentener, F.J., Dlugokencky, E.J., Easterling, D.R., Kaplan, A., Soden, B. J., Thorne, P.W., Wild, M., Zhai, P.M., 2013. Observations: Atmosphere and Surface. In: Stocker, T.F., Qin, D., Plattner, G.-K., Tignor, M., Allen, S.K., Boschung, J., Nauels, A., Xia, Y., Bex, V., Midgley, P.M. (Eds.), Climate Change 2013: The Physical Science Basis. Contribution of Working Group I to the Fifth Assessment Report of the Intergovernmental Panel on Climate Change. Cambridge University Press, Cambridge, United Kingdom and New York, NY, USA.

IPCC, 2014. Climate Change 2014: Synthesis Report. In: Pachauri, R.K., Meyer, L.A. (Eds.), Contribution of Working Groups I, II and III to the Fifth Assessment Report of the Intergovernmental Panel on Climate Change [Core Writing Team. IPCC, Geneva, Switzerland, p. 151.

Kane, B., Smiley, E.T., 2006. Drag coefficients and crown area estimation of red maple. Can. J. For. Res. 36, 1951–1958.

Kellomäki, S., Väisänen, H., Hänninen, H., Kolström, T., Lauhanen, R., Mattila, U., Pajari, B., 1992. SIMA: A model for forest succession based on the carbon and nitrogen cycles with application to silvicultural management of the forest ecosystem. Silva Carelica 22, 1–85.

Kellomäki, S., Peltola, H. (Eds.), 1998. Silvicultural strategies for predicting damage to forests from wind, fire and snow. University of Joensuu, Faculty of Forestry, Joensuu. Final Report of STORMS Project for years 1995–1997; EC-contract, p. 73. AIR3-CT94/2392. Research Notes.

Kitagawa, K., Iwama, S., Fukui, S., et al., 2015. Effects of components of the leaf area distribution on drag relations for cryptomeria japonica and chamaecyparis obtusa. Eur. J. For. Res. 134 (3), 403–414.
Koch, K., Samson, R., Denys, S., 2019. Aerodynamic characterisation of green wall vegetation based on plant morphology: an experimental and computational fluid dynamics approach. Biosyst. Eng. 178, 34–51.
Mayhead, G., 1973. Some drag coefficients for British forest trees derived from wind tunnel studies. Agric. Meteorol. 12, 123–130.
McPherson, E.G., van Doorn, S.S., Peper, P.J., 2016. Urban tree database and allometric equations. General Technical Reports. U.S. Department of Agriculture, Forest Service, Pacific Southwest Research Station, Albany, CA, p. 86. PSW-GTR-253.
N. US Department of Commerce. 2023 Global monitoring laboratory - carbon cycle greenhouse gases. https://gml.noaa.gov/ccgg/trends/ (accessed 18 March 2022).
Peltola, H.M., 2006. Mechanical stability of trees under static loads. Am. J. Bot. 93, 1501–1511.
Poorter, H., Navas, M.L., 2003. Plant growth and competition at elevated CO_2: on winners, losers and functional groups. New Phytol. 157 (2), 175–198. https://doi.org/10.1046/j.1469-8137.2003.00680.x.
Romanic, D., Hangan, H., Ćurić, M., 2018. Wind climatology of toronto based on the NCEP/NCAR reanalysis 1 data and its potential relation to solar activity. Theor. Appl. Climatol. 131, 827–843.
Seneviratne, S.I., Nicholls, N., Easterling, D., Goodess, C.M., Kanae, S., Kossin, J., Luo, Y., Marengo, J., McInnes, K., Rahimi, M., Reichstein, M., Sorteberg, A., Vera, C., Zhang, X., 2012. Changes in climate extremes and their impacts on the natural physical environment. In: Barros, V., Stocker, T.F., Qin, D., Dokken, D.J., Ebi, K.L., Mastrandrea, M.D., Mach, K.J., Plattner, G.-K., Allen, S.K., Tignor, M., Midgley, P.M. (Eds.), Managing the Risks of Extreme Events and Disasters to Advance Climate Change Adaptation, Field, C.B. Cambridge University Press, Cambridge, UK, and New York, NY, USA, pp. 109–230. A Special Report of Working Groups I and II of the Intergovernmental Panel on Climate Change (IPCC).
Taylor, H., 2022. Insurance Claims Information – January 01, 2017 to December 31, 2021. https://www.toronto.ca/wp-content/uploads/2022/02/8c76-Claim-Disclosure-Report-2021Final-FINAL.pdf (accessed 7 June 2022).
van Schooten, J.P., 1985. Fysische aspecten van windworp bij de douglasspar, Vakgroep Bosteelt. Landbouwhogeschool, Wageningen, the Netherlands, p. 200.
Yan, L., Xu, X., Xia, J., 2019. Different impacts of external ammonium and nitrate addition on plant growth in terrestrial ecosystems: a meta-analysis. Sci. Total Environ. 686, 1010–1018.
Wang, D., Heckathorn, S.A., Wang, X., Philpott, S.M., 2012. A meta-analysis of plant physiological and growth responses to temperature and elevated CO_2. Oecologia 169 (1), 1–13.